2019 IEEE 16th International Symposium on Biomedical Imaging (ISBI 2019)
Venice, Italy, April 8-11, 2019

ACCESSING LATENT CONNECTOME OF MILD COGNITIVE IMPAIRMENT VIA DISCRIMINANT STRUCTURE LEARNING

Li Wang[1], Lu Zhang[2], Dajiang Zhu[2]

[1] Mathematics, University of Texas at Arlington, Arlington, TX, USA
[2]Computer Science and Engineering, University of Texas at Arlington, Arlington, TX, USA

ABSTRACT

For decades, many potential measures have been proposed and examined in terms of their predicting capability for mild cognitive impairment (MCI). The development of non-invasive markers from multiple imaging modalities including MRI (T1-wighted), diffusion tensor imaging and functional MRI are of great interest. However, most of previous studies focused on classification, prediction or identification of statistical differences among different groups (Normal controls, MCI/AD) and clinical stages (longitudinal studies). It is still largely unknown whether there exists a way to quantitatively model the entire progression process of the disorder. Here we introduced a novel supervised discriminant structure learning method to explore latent structures of both structural and functional connectome of MCI patients. Our result shows that a latent structure reflecting the entire progression process of MCI can be learned from both structural and functional connectome. When considering more connectome features, the learned structure using functional data tend to display more heterogeneous patterns.

Index Terms— fMRI, DTI, Alzheimer's Disease, structural learning

1. INTRODUCTION

Unlike other medical conditions, the greatest known risk factor of AD is increasing age [1]. Given the fact that reversing the pathology of AD may prove to be impossible, a more tractable goal may be the prevention or slowing of the disease when diagnosed in its earliest or even pre-stage, such as mild cognitive impairment (MCI) [2]. MCI is considered as the precursor of AD and converts to AD at approximately 10% to 15% per year [3]. The future of healthcare for AD/MCI lies in its early diagnosis/treatment and progression monitoring. Comparing to amyloid PET [4-5] and FDG PET [6], non-invasive imaging modalities including structural MRI (T1-weighted) [7, 22], diffusion tensor imaging (DTI) [8, 21], resting state fMRI (rsfMRI) [9-10] or their combination [25] are poised to play an increasingly important role in the development of early imaging markers for AD/MCI. Despite the tremendous advancements made by these computational methodologies, they only focused on classification/prediction or identification of statistical differences among different groups (normal controls-NC, MCI, AD) and clinical stages (longitudinal studies). It is still largely unknown whether there exists a way to quantitatively model the entire MCI progression process.

Here, instead of focusing on isolated structural and/or functional alterations (e.g. gray matter atrophy, white matter disruption and abnormal functional connectivity) between NC and MCI/AD patients, we introduced a novel framework to quantitatively model the entire progression process of MCI via a novel discriminant structure learning method. Unlike group ICA [11] and sparse learning [24] that tend to find a set of common basis for representing the original data, our method aims to identify a latent structure space that the differences across multiple groups can be maximized. The difference between our method and other projection based methods is that the latent structure learning is automatic and the learned optimal discriminant structure can be arbitrary structures (e.g. a tree) which is purely based on input data. In this work, we applied our method to the multi-modality dataset from Alzheimer's Disease Neuroimaging Initiative (ADNI) [12], including 160 participants coming from four groups: NC, significant memory concern (SMC), early mild cognitive impairment (EMCI), and late mild cognitive impairment (LMCI). ***Fig. 1*** summarizes the major steps of our method.

All 160 subjects involved in this work have T1-weighted, DTI and rsfMRI data available. After standard preprocessing, we registered both T1-weighted and rsfMRI data to DTI space for joint modeling. We adopted Desikan-Killiany atlas [20] (middle of ***Fig. 1 (a)***) which will parcellate the cerebral cortex into 68 regions (34 for each hemisphere). We generate both structural and functional connectome based on white matter connectivity strength and correlations between BOLD signals, respectively. Then we conducted a novel discriminant structure learning method (***Fig. 1 (b)***) to the connectome to explore the optimal structures that can effectively represent the relations among different groups (***Fig. 1 (c)***). Interestingly, for both structural and functional connectome, we successfully identified a consistent structure that reflects a virtual "path": it starts from normal, goes through SMC and EMCI, and eventually ends with LMCI. In addition, our results indicate that structural connectome derived latent structures are relatively consistent. Using functional connectome, however,

978-1-5386-3640-4/19/$31.00 ©2019 IEEE

the learned structures show more heterogeneity when considering more connectome features.

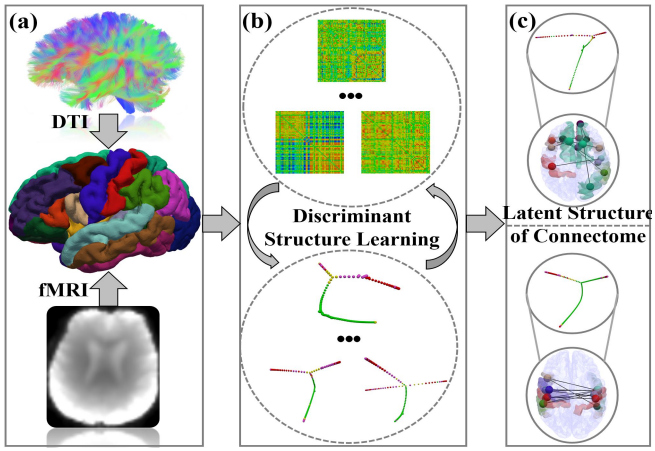

Fig.1. Overview of our proposed framework. **(a)** Joint modeling of multiple modalities including T1-weighted, DTI and rsfMRI data. **(b)** Generating brain structural and functional connectome based on atlas and conducting discriminant structure learning. **(c)** The leaned discriminant structures for structural and functional connectome.

2. METHODS

2.1. Data acquisition and preprocessing

The dataset used in this work was obtained from ADNI [12]. Originally we have a total of 473 participants. Only 160 subjects (94 NC, 13 SMC, 24 EMCI and 29 LMCI patients) have all three modalities (T1, DTI and rsfMRI) at the time we conducted the analysis. For T1 data, the imaging is 1.0mm isotropic, TE=2.98ms, TR=2.3s. For DTI data, the gradient direction is 54, the imaging is 2.0mm isotropic, TE=56ms, TR=7.2ms. For rs-fMRI data, the range of imaging resolution in X and Y dimensions is from 2.29mm to 3.31mm. The slice thickness is 3.31mm. TE=30ms and TR is from 2.2s to 3.1s. There are 140 volumes for each participant.

Standard preprocessing procedures have been applied to all modalities. More information on acquisition, preprocessing and connectome construction may be found in [2, 10]. We registered both T1 and rsfMRI to DTI space using FLIRT [23] and adopted Desikan-Killiany atlas [20] for connectome reconstruction.

2.2. Discriminant structure learning

We conduct discriminant structure learning for brain structural and functional connectome separately. It includes two steps: Firstly, we adopt a supervised feature selection method, Laplacian score [13], to alleviate the potential influence of noise and obtained a set of relevant features. Secondly, we propose a novel discriminant structure learning strategy to learn the structure over the latent space.

2.2.1. Supervised feature selection

Let $X \in \mathbb{R}^{N\times D}$ be the connectome data, where N is the number of participants and D is the number of features (2278 in this work). Assume that X is generated from an unknown distribution with certain noise, so it is important to extract relevant signals before learning the latent structures. Supervised Laplacian score [13], as a pre-step before structure learning, is very efficient for selecting relevant features from data in a high-dimensional space. It aims to rank all features based on the geometry structure of the manifold. Often the k-nearest neighbor graph G is constructed from X used for approximating the manifold. Accordingly, the importance of a feature can be measured by the degree of the matching between the data sampled from the feature and the graph structure. Let W be the weight matrix of G with the (i,j)th entry $w_{i,j}$ for the connectivity between two points x_i and x_j, and f_r be the rth feature vector denoted by the rth column of X. The Laplacian score of the rth feature is defined as

$$ls(r) = \frac{\tilde{f}_r^T L \tilde{f}_r}{\tilde{f}_r^T D_W \tilde{f}_r}, \quad (1)$$

where $L = D_W - W$ is the graph Laplacian matrix over G, $D_W = \mathrm{diag}(W\mathbf{1})$, $\mathbf{1}$ is the column vector of all ones, and

$$\tilde{f}_r = f_r - \frac{f_r^T D_W \mathbf{1}}{\mathbf{1}^T D_W \mathbf{1}}\mathbf{1}. \quad (2)$$

The smaller $ls(r)$ is, the more important the rth feature is. Hence, features can be ordered in terms of the importance according to the Laplacian score.

Since the Laplacian score is defined on a given graph, it becomes critical to construct a graph that can faithfully represent the underlying manifold structure of data. Ordered label information is useful to construct a proper graph. Denote the labels of data X by $\boldsymbol{y} = [y_1, \dots, y_N] \in \{1,2, \dots, c\}^N$ where there are c classes in total. Without the loss of generality, the ordering of the labels is defined as $1 < 2 < \cdots < c$. Two types of graphs are constructed as follows. The within-class graph is defined to capture the relationship between data points of the same class as

$$W_{i,j}^c = \begin{cases} 1, & y_i = y_j \\ 0, & \text{otherwise} \end{cases}, \quad (3)$$

And, the ordering of the class labels is encoded to model the relationship of two points in-between two classes of the closest neighbors, given by

$$W_{i,j}^o = \begin{cases} 1, & |y_i - y_j| = 1 \ \textit{and} \ (j \in \mathcal{N}_i \ \textit{or} \ i \in \mathcal{N}_j) \\ 0, & \text{otherwise} \end{cases}, \quad (4)$$

where $\mathcal{N}_i$ is the set of indices of data points that are the neighbors of x_i in the neighbor graph G. Finally, the weight matrix used in (1) is defined as $W = W^c + W^o$, which naturally incorporates ordering label information. By using the constructed weight matrix, the Laplacian score can be used for selecting a set of features that can preserve the ordering label information provided by the data.

2.2.2. Latent structure learning with supervision

Recently, a tree structure learning algorithm named as DDRTree [14] has been proposed and successfully applied to fMRI data [15]. Since DDRTree is an unsupervised learning approach, it is less robust to obtain the proper embedded points that can maintain the ordering of class labels along the learned graph structure. In [15], class information has been explored to alleviate above issue, but it is used to select a subset of instances according to clustering results as a preprocessing step for DDRTree. Moreover, the overlapping region on the graph have not been explored in [15]. Here, we proposed a novel unified model with supervised setting to overcome the drawback of DDRTree for learning a graph structure in a latent space, so that the learned structure is consistent with the label ordering information of the data.

Supervised dimensionality reduction approaches have been widely studied in the literature, including linear discriminant analysis [16] and graph embedding [17]. These methods [16-17] aim to best characterize the similarity relationship between pairs of data points. In graph embedding, the graph preserving criterion is formulated to learn embedded points $Z \in \mathbb{R}^{N\times d}$ by solving the following minimization problem

$$\min Tr(Z^T AZ):\ Z^T BZ = I, \tag{5}$$

where A is the Laplacian matrix, B is the constraint matrix, and the dimension $d \le D$. Most of these methods are specifically designed for classification problem based on the assumption that data points in the same class should be as close as possible in the embedding space, while data points with different classes are far away from each other. Hence, the existing methods are not well suitable for learning graph structure that allows overlapping regions among data points of different classes to characterize the evolutionary progression such as progression process of MCI (NC-SMC-EMCI-LMCI). Moreover, the graph constructed from the original data might be suboptimal to approximate the inherent graph in the latent space.

In this work, we propose a new model to overcome the above issues. First, we reformulate (5) by properly defining matrices A and B to capture the initial graph structure based on the rough estimation from the original data. And then, the initial structure is updated gradually to capture the inherent structure of the data via graph learning criterion.

Given a neighborhood graph G, we have $\mathcal{N}_i$ as the set of indices of data points that are the neighbors of x_i. Let W^{ng} be the contingency matrix of G, that is,

$$W_{i,j}^{ng} = \begin{cases} 1, & j \in \mathcal{N}_i \ or \ i \in \mathcal{N}_j \\ 0, & \text{otherwise} \end{cases}, \tag{6}$$

A within-class weight matrix W^{wc} is defined to capture the data points that are in the same class and also neighbors of each other, given by

$$W_{i,j}^{wc} = \begin{cases} 1, & \left(j \in \mathcal{N}_i \ or \ i \in \mathcal{N}_j\right) and \ y_i = y_j \\ 0, & \text{otherwise} \end{cases}. \tag{7}$$

Let $W_A = (1-\alpha)W^{wc} + \alpha W^o$ and $W_B = W^{ng} - W^{wc} - W^o$. By the definition of graph Laplacian matrix, we have that $A = diag(W_A\mathbf{1}) - W_A$ and $B = diag(W_B\mathbf{1}) - W_B$, where α is a parameter for controlling the volumes of overlapping regions among different classes. Instead of solving problem (5) in the graph embedding framework, we propose to solve the following regularization problem with a stable numerical solution given by

$$\min Tr(Z^T(B+\gamma I)^{-1}AZ):\ Z^T Z = I, \tag{8}$$

where γ is a regularization parameter.

The reversed graph embedding approach [14] is used for learning graph structures in a latent space from high-dimensional data. Let S be a matrix variable where each entry represents the connectivity of two embedded points. In other word, the structure we would like to learn is controlled by the nonzero elements in matrix S. With the ordering label information as the guide, the novel latent structure learning is formulated as the following joint minimization problem

$$\min_{Z,S} Tr(Z^T(B+\gamma I)^{-1}AZ) + \beta \sum_i \sum_j s_{i,j}\left\|z_i - z_j\right\|^2 \tag{9}$$
$$s.t.\ Z^T Z = I,$$
$$S \in \mathcal{G},$$

where $\mathcal{G}$ is a feasible set of all specific types of graphs (e.g. spanning tree), and β is a parameter to trade off the supervised dimensionality reduction and reversed graph embedding. Problem (9) can be efficiently solved by the alternating method. For a fixed Z, we need to solve the following optimization problem with a matrix variable S:

$$\min_{S\in\mathcal{G}} \sum_i \sum_j s_{i,j}\left\|z_i - z_j\right\|^2, \tag{10}$$

where $\mathcal{G}$ is the set of matrices that can represent minimum cost spanning trees where the cost is defined as the Euclidean distance between two embedded points. Hence, problem (10) can be solved efficiently by Kruskal's algorithm [18]. For a fixed S, problem (9) with respect to Z is reduced to the eigen-decomposition problem, where the eigenvectors associated to the d smallest eigenvalues are concatenated to form the optimal solution of Z.

3. RESULTS

We applied the above-mentioned method to brain structural and functional connectome of 160 subjects in ADNI. Section 3.1 shows the learned structures using top 10 connectome features. Reproducibility results with different connectome features are shown in section 3.2.

3.1. Whole brain structure learning

We applied our method on structural and functional connectome independently. ***Fig. 2(a)*** shows the learned latent structure from 160 structural connectomes using top 10 connectivity features that show the best discriminant capabilities. Bubbles with different colors represent different groups and each bubble is the projection of a single subject. In general, this learned structure "grows" from NC subjects (green) to SMC (yellow) and extends into two branches. Each branch goes through EMCI (pink) and ends with LMCI (red). ***Fig. 2(b)*** indicates the structure learned from functional connectome.

The overall structure is consistent with structural one and the only difference is that there are three branches learned using functional data instead of two with structural data. The patterns of progression (NC-SMC-EMC-LMCI) are consistent within both learned structures. The top 10 connectome features used are shown in ***Fig. 2(c-d)*** and the names in atlas are shown in ***Table. 1***. Each sub-figure has two rows: the involved brain regions are shown in the top and the bottom illustrates the used connectivity (each bubble is corresponding to the regions in the top with the same color). One interesting observation is that the most discriminant structural connectome are not necessarily consistent with functional ones, but some regions tend to be involved in both structural and functional learning through all MCI progression stages, such as superior-temporal and postcentral gyrus.

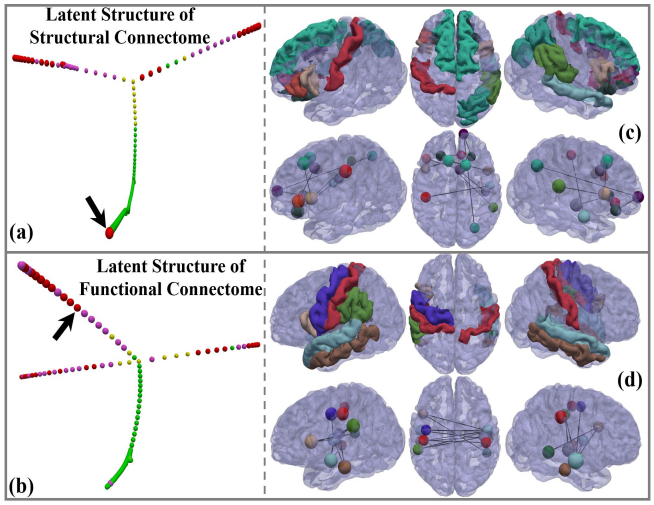

Fig.2. (a-b) the learned discriminant structures using structural and functional connectome, respectively. Different colors represent different groups: NC (green), SMC (yellow), EMCI (pink) and LMCI (red). Each bubble is a projection of a single subject. **(c-d)** the top 10 connectome features used to learn the latent structure. **Top**: the involved brain regions. **Bottom**: the connectivity between these regions and each bubble is corresponding to the regions with the same color in the top.

Structural Connectome	Functional Connectome
l.supfrontal-r.supfrontal	**l.suptemporal**-r.midtemporal
l.tratemporal-**r.latorbfrontal**	**l.suptemporal**-r.supramarginal
l.medorbfrontal-**r.latorbifrontal**	l.postcentral-r.postcentral
l.suptemporal-r.postcentral	**l.suptemporal**-r.suptemporal
l.supramarginal-**r.latorbifrontal**	**l.suptemporal**-r.precentral
l.supparietal-l.frontalpole	l.tratemporal-r.midtemporal
r.parsopercularis-r.supfrontal	**l.suptemporal**-r.parsopercularis
l.latorbifrontal-l.frontalpole	l.tratemporal-r.supramarginal
l.caudantcin-r.parstriangularis	l.midtemporal-r.suptemporal
l.parsopercularis-l.supfrontal	l.bankssts-r.parsopercularis

Table. 1. Top 10 connectome features used to learn discriminant structures. The highlighted brain regions have the most frequency of appearance in the used connectome.

In ***Fig. 2*** we highlighted one subject (labeled as LMCI in ADNI) who is located in NC range within structural space but in LMCI range within functional space. This suggests that the functional abnormality might happen before structural alterations [19].

3.2. Discriminant structure learning using different size of connectome features

Section 3.1 shows the learned structures using top 10 connectome features. To explore the relations between the learned structures and the number of connectome features used, we conducted the same learning process with top 20, 50 and 100 features and the results are shown in ***Fig. 3***. The structures in top and bottom are learned from structural and functional connectome, respectively. Though we used different number of connectome features to learn the latent structure, we can see that for structural connectome, we can always achieve a relatively consistent and stable structure: it starts from NC, extends to SMC, EMCI and ends with LMCI (***Fig.3 (a-d) top***). For structures learned from functional connectome, the latent structures tend to be more complicate with more connectome features considered (***Fig.3 (a-d) bottom***). For example, the bottom of ***Fig. 3(d)*** shows the functional result using 100 connectome features and the learned structure displays a heterogeneous pattern within NC.

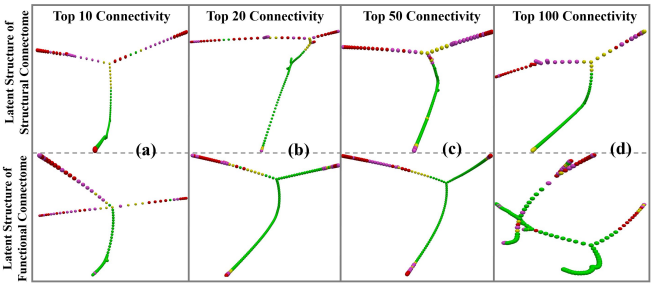

Fig. 3. The discriminant structures learned using top 10 **(a)**, 20 **(b)**, 50 **(c)** and 100 **(d)** connectome features. **Top** and **bottom** show the results derived from structural and functional connectome, respectively.

4. CONCLUSION

Here we proposed a novel framework to learn discriminant structure information from both structural and functional data coming from multiple populations (NC, SMC, EMCI and LMCI). Different from previous prediction and classification studies, we aim to learn a latent structure that can reflect the entire process of MCI progression. Our results show that a consistent progression pattern can be learned from both structural and functional connectome. This structure is relatively stable in structural space, but display more heterogeneous patterns when considering more connectome features.

5. REFERENCES

[1] Hebert, L. E., Weuve, J., Scherr, P. A. and Evans, D. A. "Alzheimer disease in the United States (2010-2050) estimated using the 2010 census," *Neurology*, 80(19), pp.1778–1783, 2013.

[2] Dajiang Zhu, Kaiming Li, Douglas P. Terry, A. Nicholas Puente, Lihong Wang, Dinggang Shen, L. Stephen Miller, and Tianming Liu. "Connectome- scale assessments of structural and functional connectivity in MCI," *Human brain mapping*, 35(7), pp.2911-2923, 2014.

[3] M. Grundman, R.C. Petersen, S.H. Ferris, R.G. Thomas, P.S. Aisen, D.A. Bennett, N.L. Foster, C.R. Jack Jr, D.R. Galasko, R. Doody, and J. Kaye, "Mild cognitive impairment can be distinguished from Alzheimer disease and normal aging for clinical trials," *Archives of neurology*, 61(1), pp.59–66, 2004.

[4] W.E. Klunk, H. Engler, A. Nordberg, Y. Wang, G. Blomqvist, D.P. Holt, M. Bergström, I. Savitcheva, G.F. Huang, S. Estrada, and B. Ausén, "Imaging brain amyloid in Alzheimer's disease with Pittsburgh Compound-B," *Annals of Neurology: Official Journal of the American Neurological Association and the Child Neurology Society.* 55(3), pp.306–319, 2004.

[5] C.C. Rowe, K.A. Ellis, M. Rimajova, P. Bourgeat, K.E. Pike, G. Jones, J. Fripp, H. Tochon-Danguy, L. Morandeau, G. O'Keefe, and R. Price, "Amyloid imaging results from the Australian Imaging, Biomarkers and Lifestyle (AIBL) study of aging," *Neurobiology of aging*, 31(8), pp.1275–1283, 2010.

[6] W.J. Jagust, D. Bandy, K. Chen, N.L. Foster, S.M. Landau, C.A. Mathis, J.C. Price, E.M. Reiman, D. Skovronsky, R.A. Koeppe, and Alzheimer's Disease Neuroimaging Initiative, "The Alzheimer's Disease Neuroimaging Initiative positron emission tomography core," *Alzheimer's & Dementia*, 6(3), pp.221–9, 2010.

[7] L. Wang, F.C. Goldstein, E. Veledar, A.I. Levey, J.J. Lah, C.C. Meltzer, C.A. Holder, and H. Mao, "Alterations in cortical thickness and white matter integrity in mild cognitive impairment measured by whole-brain cortical thickness mapping and diffusion tensor imaging," *American Journal Of Neuroradiology*, 30(5), pp. 893–899, 2009.

[8] C.Y. Wee, P.T. Yap, W. Li, K. Denny, J.N. Browndyke, G.G. Potter, K.A. Welsh-Bohmer, L. Wang, and D. Shen, "Enriched white matter connectivity networks for accurate identification of MCI patients," *Neuroimage*, 54(3), pp.1812–1822, 2011.

[9] M.D. Greicius, G. Srivastava, A.L. Reiss, and V. Menon, "Default-mode network activity distinguishes Alzheimer's disease from healthy aging: evidence from functional MRI," *PNAS*. 101(13), pp.4637–4642, 2004.

[10] X. Jiang, X. Zhang, D. Zhu, and Alzheimer's Disease Neuroimaging Initiative. "Intrinsic functional component analysis via sparse representation on Alzheimer's disease neuroimaging initiative database," *Brain* connectivity, 4(8), pp.575-586, 2014.

[11] V. Calhoun, T. Adali, G. Pearlson, and J. Pekar, "A method for making group inferences using independent component analysis of functional MRI data: Exploring the visual system," *Neuroimage*, 13(6), pp.88-88, 2001.

[12] http://adni.loni.usc.edu/

[13] X. He, D. Cai, and P, "Niyogi Laplacian score for feature selection," In *Advances in neural information processing systems*, pp. 507-514, 2006.

[14] L. Wang and Q. Mao, "Probabilistic dimensionality reduction via structure learning," *IEEE Transactions on Pattern Analysis and Machine Intelligence*, 2017.

[15] D. Zhu, and L. Wang, "Exploring latent structures of Alzheimer's disease via structure learning," In *Biomedical Imaging (ISBI 2018), 2018 IEEE 15th International Symposium on*, pp. 536-540, 2018.

[16] R. O. Duda, P. E. Hart, and D. G. Stork, *Pattern classification*. John Wiley & Sons, 2012.

[17] S. Yan, D. Xu, B. Zhang, and H. J. Zhang, "Graph embedding: A general framework for dimensionality reduction," *CVPR. IEEE Computer Society Conference on,* pp. 830-837, 2005.

[18] M. Cheung, "Minimum-cost spanning trees." https://people.orie.cornell.edu/dpw/orie6300/fall2008/Recitations/rec09.pdf

[19] F. Palesi, G. Castellazzi, L. Casiraghi, E. Sinforiani, P. Vitali, C.A. Gandini Wheeler-Kingshott, and E. D'Angelo, "Exploring patterns of alteration in Alzheimer's disease brain networks: a combined structural and functional connectomics analysis," *Frontiers in neuroscience*, 10, p.380, 2016.

[20] R.S. Desikan, F. Ségonne, B. Fischl, B.T. Quinn, B.C. Dickerson, D. Blacker, R.L. Buckner, A.M. Dale, R.P. Maguire, B.T. Hyman, M.S. Albert, "An automated labeling system for subdividing the human cerebral cortex on MRI scans into gyral based regions of interest," *Neuroimage*, 31(3) pp.968-980, 2006.

[21] G. Douaud, S. Jbabdi, T.E. Behrens, R.A. Menke, A. Gass, A.U. Monsch, A. Rao, B. Whitcher, G. Kindlmann, P.M. Matthews, S. Smith."DTI measures in crossing-fibre areas: increased diffusion anisotropy reveals early white matter alteration in MCI and mild Alzheimer's disease," *Neuroimage* , 55(3), pp.880-890, 2011.

[22] G. Chetelat, B. Landeau, F. Eustache, F. Mezenge, F. Viader, V. De La Sayette, B. Desgranges, and J-C. Baron, "Using voxel-based morphometry to map the structural changes associated with rapid conversion in MCI: a longitudinal MRI study," *Neuroimag*, 27(4), pp. 934-946, 2005.

[23] https://fsl.fmrib.ox.ac.uk/fsl/fslwiki/FLIRT

[24] J. L, X. Jiang, X. Li, D. Zhu, S. Zhang, S. Zhao, H. Chen, T. Zhang, X. Hu, J. Han, and J. Ye, "Holistic atlases of functional networks and interactions reveal reciprocal organizational architecture of cortical function," *IEEE Transactions on Biomedical Engineering*, 62(4), pp.120-1131, 2015.

[25] D. Zhu, T. Zhang, X. Jiang, X. Hu, H. Chen, N. Yang, J. Lv, J. Han, L. Guo, and T. Liu, "Fusing DTI and fMRI data: a survey of methods and applications," *NeuroImage*, 102, pp.184-191, 2014.